PCCP

ROYAL SOCIETY OF CHEMISTRY

PAPER

View Article Online
View Journal | View Issue



Cite this: *Phys. Chem. Chem. Phys.*, 2023, **25**, 4754

# Insights into the molecular structure and infrared spectrum of the prebiotic species aminoacetonitrile†

Ningjing Jiang, [a] Mattia Melosso, *[b] Silvia Alessandrini, [ac] Luca Bizzocchi,[a] Marie-Aline Martin-Drumel, [d] Olivier Pirali[de] and Cristina Puzzarini *[a]

Received 4th November 2022,
Accepted 17th January 2023

DOI: 10.1039/d2cp05179f

rsc.li/pccp

Aminoacetonitrile is an interstellar molecule with a prominent prebiotic role, already detected in the chemically-rich molecular cloud Sagittarius B2(N) and postulated to be present in the atmosphere of the largest Saturn's moon, Titan. To further support its observation in such remote environments and laboratory experiments aimed at improving our understanding of interstellar chemistry, we report a thorough spectroscopic and structural characterization of aminoacetonitrile. Equilibrium geometry, fundamental bands as well as spectroscopic and molecular parameters have been accurately computed by exploiting a composite scheme rooted in the coupled-cluster theory that accounts for the extrapolation to the complete basis set limit and core-correlation effects. In addition, a semi-experimental approach that combines ground-state rotational constants for different isotopic species and calculated vibrational corrections has been employed for the structure determination. From the experimental side, we report the analysis of the three strongest fundamental bands of aminoacetonitrile observed between 500 and 1000 $cm^{-1}$ in high-resolution infrared spectra. More generally, all computed band positions are in excellent agreement with the present and previous experiments. The only exception is the $\nu_{15}$ band, for which we provide a revision of the experimental assignment, now in good agreement with theory.



## 1 Introduction

Over the past 50 years, a wide number of interstellar amino acids have been discovered in extraterrestrial objects, including meteorites,[1–5] asteroids,[6] and comets.[7,8] However, despite extensive and dedicated searches, no evidence of amino acids in the gas phase of the interstellar medium (ISM) has been found to date.[9,10] Yet, several molecular precursors of amino acids – and progenitors of biological species in general – have been discovered in the ISM in recent years, including for example aminoacetonitrile,[11] glycolaldehyde,[12] ethenediol,[13] ethanolamine,[14] hydroxylamine,[15] urea,[16,17] formamide,[18] and many others. Among these, aminoacetonitrile is one of the closest glycine precursors and has been observed in the high-mass star-forming region Sagittarius B2(N).[11,19,20]

Aminoacetonitrile is regarded as a prebiotic species because it is formed as intermediate in the second step of the Strecker synthesis of glycine, a chemical process based on simple reactants such as ammonia, formaldehyde, and hydrogen cyanide.[21] The efficiency of this process in producing aminoacetonitrile even in astrophysical-like conditions has been demonstrated by Danger *et al.*,[22] who monitored the products released during the warm-up of interstellar ice-analogues containing the ingredients of the Strecker synthesis without the involvement of VUV photons or any energetic particles. A subsequent experimental study, though, has shown that the hydrolysis of aminoacetonitrile to glycine (*i.e.* the last two steps of the Strecker synthesis) is unfeasible under the same conditions,[23] as already predicted computationally.[24] Moreover, aminoacetonitrile has been shown to be photoresistant to VUV radiation and to possess a high desorption energy, thus making it one of the most important reservoir of interstellar glycine.[23] Nonetheless, this reservoir could have been present in asteroids and delivered to the aqueous phase of the early Earth during the

[a] *Dipartimento di Chimica "Giacomo Ciamician", Università di Bologna, Via F. Selmi 2, 40126 Bologna, Italy. E-mail: cristina.puzzarini@unibo.it*
[b] *Scuola Superiore Meridionale, Largo San Marcellino 10, 80138 Naples, Italy. E-mail: mattia.melosso@unina.it*
[c] *Scuola Normale Superiore, Piazza dei Cavalieri 7, 56126 Pisa, Italy*
[d] *Université Paris-Saclay, CNRS, Institut des Sciences Moléculaires d'Orsay, 91405 Orsay, France*
[e] *SOLEIL Synchrotron, AILES beamline, l'Orme des Merisiers, 91190 Saint-Aubin, Gif-sur-Yvette, France*

† Electronic supplementary information (ESI) available: List of the transitions assigned for the $\nu_8$, $\nu_9$, $\nu_{10}$ bands; geometry and harmonic frequencies at the HF-SCF level; vibration–rotation interaction constants at the MP2 level. See DOI: https://doi.org/10.1039/d2cp05179f

late heavy bombardment period,[25] where the hydrolysis process of aminoacetonitrile could have taken place and formed glycine.

In addition to the Strecker synthesis, the formation of aminoacetonitrile in interstellar conditions has been observed during the VUV irradiation of an acetonitrile/ammonia ice mixture[26] as well as after the heating of acetonitrile-rich ices previously irradiated by X-rays,[27] in accordance with chemical models.[28] Furthermore, aminoacetonitrile has been identified among the components of Titan aerosol analogs produced in the laboratory by discharging a 95 : 5 mixture of $N_2$ and $CH_4$ in a high vacuum reaction chamber at 195 K.[29] This result points out the importance of aminoacetonitrile not only in hot molecular cores but also in Titan's atmosphere.

Given its importance in a variety of astrophysical objects, it is evident that a thorough spectroscopic characterization of aminoacetonitrile is mandatory in order to support its observation. If, on the one hand, ISM detections typically rely on the observation of rotational transitions at centimeter-/millimeter-wavelengths,[30] on the other hand observations of planetary atmospheres and many laboratory studies (such as those mentioned above) are mainly based on the identification of vibrational features in the infrared domain.

The rotational spectrum of aminoacetonitrile has been investigated extensively. Previous works include the study of the vibrational ground state[31–33] and several excited states[34,35] of the main isotopic species, the observation of some isotopologues,[31,33,34,36] the analysis of the hyperfine structure produced by the two nitrogen nuclei,[37] and the determination of dipole moment components.[36] Conversely, the vibrational spectrum has been studied mainly at low resolution, either in the gas phase[38] or in Ar matrix,[39] with only three fundamental bands analyzed at high resolution.[20] Moreover, the vibrational analysis is still ambiguous and suffers from a limited support by quantum chemistry, so far restricted to low-level calculations.[39–41]

More generally, no study has properly addressed a complete structural and spectroscopic characterization of aminoacetonitrile using high-level quantum-chemical calculations. Here, we want to fill this gap and to expand the knowledge of the high-resolution rovibrational spectrum of aminoacetonitrile in the region between 500 and 1000 $cm^{-1}$. To reach our goals, we combined a high-level quantum-chemical characterization of its structure and spectroscopic properties with the analysis of high-resolution infrared spectra recorded at the AILES beamline of SOLEIL synchrotron. More specifically, the goals of our work can be summarized as follows: (i) to derive a semi-experimental equilibrium structure of aminoacetonitrile and compare it with our best theoretical estimate; (ii) to carry out a theoretical rotational spectroscopic characterization; (iii) to predict the position of all fundamental bands with high accuracy and compare it with experimental data; (iv) to analyze the rotational structure of three new fundamental bands supported by computed vibration–rotation interaction constants.

## 2 Experimental details

The gas-phase infrared spectrum of aminoacetonitrile has been recorded between 500 and 1500 $cm^{-1}$ using the Bruker IFS 125 FT interferometer located at the AILES beamline of the SOLEIL synchrotron facility.[42] For this purpose, the spectrometer has been equipped with a White-type cell adjusted to attain an optical path length of about 150 m,[43,44] a globar lamp as infrared radiation source, a KBr beamsplitter, and a MCT detector.[45] The iris aperture was set to 1.15 mm, thus allowing for a spectral resolution of 0.0015 $cm^{-1}$ in the entire frequency range (the Doppler broadening at these wavenumbers is smaller than $3 \times 10^{-4}$ $cm^{-1}$). Two diamond windows were used to isolate the cell from the interferometer, which was kept evacuated under continuous pumping to limit the absorption of atmospheric water. Aminoacetonitrile has been injected inside the cell at a pressure of 3 μbar to limit the saturation of the intense $\nu_9$ band at $\sim$790 $cm^{-1}$.

The final spectrum consists of 112 individual scans, co-added in order to improve its signal-to-noise ratio. After the baseline removal, the spectrum was calibrated using infrared bands of two interfering species, namely HCN and $CO_2$. The HCN frequencies were taken from the HITRAN2020 database,[46] while those of the $CO_2$ band around 670 $cm^{-1}$ were taken from ref. 47. No apodization functions were applied to the interferograms.

## 3 Computational details

Quantum-chemical calculations have been performed at different levels of theory, with the aim of obtaining the best possible estimates for the molecular geometry, vibrational frequencies, rotational and centrifugal distortion constants, electric dipole moment, and nuclear quadrupole coupling constants. The computational methodology employed is summarized in the following.

The so-called CBS+CV scheme[48–51] has been employed for an accurate determination of the equilibrium structure and harmonic force field. This approach involves calculations at the coupled cluster (CC) singles and doubles with perturbative triples corrections (CCSD(T)) level[52] and relies on the additivity approximation:

$$p_{\text{best}} = p^{\infty}(\text{HF} - \text{SCF}) + \Delta p^{\infty}(\text{CCSD(T)}) + \Delta p(\text{CV}), \quad (1)$$

where $p$ denotes a generic properties: either a structural parameter or the harmonic frequency of a given normal mode ($\omega_r$, with $r$ referring to normal modes). The first two terms on the right-hand side allow for recovering the error due to the basis-set truncation by means of an extrapolation to the complete basis set (CBS) limit, with the Hartree–Fock (HF-SCF) and CCSD(T)-correlation energy contributions extrapolated separately. For the former, the 3-point exponential formula by Feller[53] has been employed, while the 2-point expression by Helgaker and coworkers[54] has been used for CCSD(T). Since extrapolation to the CBS limit has been carried out within the frozen-core (fc) approximation, core-valence correlation (CV) effects have been incorporated by adding the corresponding difference between all-electron (ae) and fc-CCSD(T) calculations in the same basis set. The correlation-consistent polarized

cc-p(C)V$n$Z basis sets[55,56] have been employed throughout. In practical terms, geometry optimizations and the corresponding harmonic force field calculations have been performed at the HF-SCF/cc-pV$n$Z level, with $n$ = T, Q, and 5, at the fc-CCSD(T)/cc-pV$n$Z level, with $n$ = T and Q, and at the CCSD(T)/cc-pCVTZ level, both within the fc approximation and correlating all electrons (ae). As a byproduct of these geometry optimizations, first-order properties have been obtained, thus allowing the application of the CBS+CV scheme to their accurate evaluation. In the present study, the interest is on the electric dipole moment components and the electric field gradient tensor (the elements of the latter leading to the corresponding nuclear quadrupole coupling constants).[57]

From the equilibrium structure, the equilibrium rotational constants are straightforwardly derived.[57,58] While accurate CBS+CV equilibrium rotational constants and harmonic frequencies are invaluable information, for their exploitation in the field of rotational and ro-vibrational spectroscopy one needs to move from equilibrium to a realistic representation of the molecular system. This implies the incorporation of vibrational effects for rotational constants and anharmonicity for vibrational frequencies.

The vibrational dependence of the rotational constant on the vibrational state can be modelled using vibrational perturbation theory to second order (VPT2):[59]

$$B_{\mathrm{v}}^{i} = B_{\mathrm{e}}^{i} - \sum_{r} \alpha_{r}^{i}\left(v_{r} + \frac{1}{2}\right), \tag{2}$$

where $\alpha_r^i$ denotes the vibration–rotation interaction constants, with $i$ being the inertial axis ($a$, $b$ or $c$) and the sum running over all the $r$ vibrational modes ($v_r$ being the corresponding quantum number). The VPT2 model also allows for writing the vibrational fundamentals $\nu_r$ in terms of harmonic wavenumbers ($\omega_r$) and elements of the effective anharmonicity matrix ($X_{rs}$):

$$\nu_{r} = \omega_{r} + 2X_{rr} + \sum_{s\neq r=1}^{3N-6} \frac{X_{rs}}{2}. \tag{3}$$

From a computational point-of-view, evaluation of the vibration–rotation interaction constants and anharmonicity matrix elements requires the calculation of an anharmonic force field (cubic and semi-diagonal quartic force constants). This has been computed using Møller–Plesset theory to the second order (MP2)[60] in conjunction with the cc-pCVTZ basis set, with all electrons correlated. To account for resonant terms, the GVPT2 approach[61] has been employed. From anharmonic force-field calculations, as a byproduct, the sextic centrifugal distortion constants have also been obtained. Differently, the quartic centrifugal distortion terms have been derived at the CBS+CV level as a byproduct of harmonic computations.

The so-called semi-experimental (SE) approach can be used to derive an accurate equilibrium geometry ($r_{\mathrm{e}}^{\mathrm{SE}}$). This is obtained by a least-squares fit of experimental vibrational ground state rotational constants ($B_0$) of different isotopic species computationally corrected for the vibrational contribution ($\Delta B_{\mathrm{vib}}^{i}$).[57,62,63] In fact, according to eqn (2), one obtains the following expression when the vibrational ground state is considered:

$$B_{\mathrm{e}}^{i} = B_{0}^{i} + \frac{1}{2}\sum_{r} \alpha_{r}^{i} = B_{0}^{i} - \Delta B_{\mathrm{vib}}^{i}, \tag{4}$$

where, as above, $i$ refers to the inertial axis and the sum runs over all the vibrational modes.

MP2 calculations have been performed using Gaussian 16,[64] while for all the remaining calculations the CFOUR package[65,66] has been employed. While the results of all CCSD(T) calculations are reported in the main text, geometry and harmonic frequencies computed at the HF-SCF level as well as the vibration–rotation interaction constants from MP2 calculations are only provided in the ESI.†

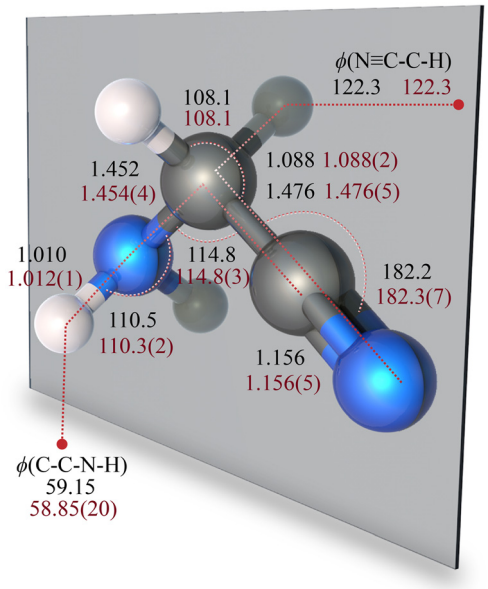


Fig. 1 Molecular structure of aminoacetonitrile together with best-estimated theoretical (CBS+CV level, in black) and semi-experimental (in dark red) equilibrium geometrical parameters. Bond lengths in Å, angles in degrees.

# 4 Results and discussion

## 4.1 Molecular structure

Previous experimental studies have shown that aminoacetonitrile only exists in the *trans* form, with the $NH_2$ moiety being opposite to the $CH_2$ group (see Fig. 1). For this reason, only this form has been investigated in this work. In its equilibrium configurations, all four heavy atoms of aminoacetonitrile lies on the same plane (the *ab* plane in its principal inertia system), with the pairs of hydrogen nuclei lying symmetrically out of this plane (see Fig. 1). Therefore, the molecule belongs to the $C_s$ point group. The existence of a $\sigma_h$ symmetry element is confirmed experimentally. For example, the absence of any *c*-type transitions in its rotational spectrum, which is instead dominated by *a*- and *b*-

 

Table 1 Structural parameters computed at different levels of theory and the semi-experimental equilibrium structure. The corresponding equilibrium rotational constants are also reported

| | CCSD(T) | | | | | | |
|---|---|---|---|---|---|---|---|
| Parameter | fc/cc-pVTZ | fc/cc-pVQZ | fc/cc-CVTZ | ae/cc-pCVTZ | CBS | CBS+CV | $r_e^{SE}$ |
| $r$(C≡N) | 1.163 | 1.160 | 1.162 | 1.160 | 1.158 | 1.156 | 1.156(5) |
| $r$(C–C) | 1.484 | 1.481 | 1.483 | 1.481 | 1.479 | 1.476 | 1.476(5) |
| $r$(C–H) | 1.090 | 1.090 | 1.090 | 1.089 | 1.089 | 1.088 | 1.088(2) |
| $r$(C–N) | 1.461 | 1.457 | 1.460 | 1.458 | 1.454 | 1.452 | 1.454(4) |
| $r$(N–H) | 1.014 | 1.012 | 1.014 | 1.012 | 1.011 | 1.010 | 1.012(1) |
| ∠(C–C≡N) | 182.4 | 182.3 | 182.4 | 182.3 | 182.2 | 182.2 | 182.3(7) |
| ∠(C–C–N) | 114.9 | 114.9 | 114.8 | 114.9 | 114.8 | 114.8 | 114.8(3) |
| ∠(C–N–H) | 109.5 | 110.0 | 109.5 | 109.6 | 110.4 | 110.5 | 110.3(2) |
| ∠(C–C–H) | 108.1 | 108.1 | 108.1 | 108.1 | 108.1 | 108.1 | 108.1 |
| $\phi$(C–C–N–H) | 57.96 | 58.54 | 57.95 | 58.11 | 59.02 | 59.15 | 58.85(20) |
| $\phi$ (N≡C–C–H) | 122.2 | 122.2 | 122.2 | 122.3 | 122.2 | 122.3 | 122.3 |
| $A_e$ | 30110.4 | 30263.4 | 30127.5 | 30228.5 | 30344.4 | 30439.4 | 30355.9 |
| $B_e$ | 4741.25 | 4757.06 | 4745.78 | 4760.21 | 4766.52 | 4781.44 | 4785.27 |
| $C_e$ | 4296.40 | 4312.59 | 4300.38 | 4313.90 | 4322.28 | 4336.05 | 4337.40 |

Bond-lengths are in Å, angles in degrees, rotational constants in MHz; fc and ae stand for frozen-core and all-electron, respectively (see text). Values in parentheses represent standard errors in unit of the last quoted digits.

type transitions,[36] demonstrates that the dipole moment component along the $c$ axis is null.

The molecular structure of aminoacetonitrile has already been investigated in the literature, both experimentally and theoretically. For what concerns experiment, the available determination only relies on the rotational constants of three different isotopologues (namely the main, –NHD, and –$ND_2$ isotopic species, which means a total of nine parameters) and does not take into account how the vibrational effects alter the molecular structure.[36] As far as computational studies are concerned, the equilibrium structure has only been calculated at low levels of theory.[40,41]

In the present study, to obtain an accurate determination of the equilibrium geometry of aminoacetonitrile, as explained in Section 3, we have carried out high-level quantum-chemical calculations and derived a semi-experimental equilibrium structure using a larger set of rotational constants with respect to previous experimental evaluations. For the $r_e^{SE}$ determination, five isotopologues have been considered, namely the main, –NHD, –$ND_2$,[33] –$^{13}CH_2$, and –$^{13}C{\equiv}N$[34] isotopic species. These provide 15 ground-state rotational constants, that are suitable for the derivation of an almost complete $r_e^{SE}$. Due to the lack of spectroscopic data for the –CHD and –$CD_2$ isotopologues, the C–H bond length and the CCH angle have been kept fixed to our best-estimated computed values, while all the remaining structural parameters have been determined during the least-squares fit. As can be seen from inspection of Table 1, the $r_e^{SE}$ values and our best-estimated CBS+CV structural parameters well agree within the statistical uncertainties of the former. Table 1 also collects the equilibrium geometries computed at different levels of theory. A monotonic trend for the CCSD(T) results by enlarging the basis set is evident, with CBS values (from the two right-hand terms of eqn (1)) being also provided in Table 1. From the comparison of the CBS and CBS+CV parameters, the importance of the CV contribution for obtaining an accuracy of about 0.001 Å for bond lengths is also apparent. For angles, the error affecting the CBS+CV structure is about 0.1°. The quality of the $r_e^{SE}$ geometry is well assessed not only by the small uncertainties, but also by the fact that the experimental rotational constants of all isotopologues are reproduced with a standard deviation of 1.6 MHz for the $A$ constant and of 0.1 MHz for $B$ and $C$.

Finally, in Table 1, the equilibrium rotational constants corresponding to the various structures reported are provided. These data allow us to point out the importance of applying a composite scheme to reproduce experimental rotational constants.

### 4.2 Rotational parameters

The rotational spectrum of the main isotopologue of aminoacetonitrile has been investigated extensively in the literature. Although experimental studies span from the centimeter-wave region to the millimeter-wave and THz domains, the spectroscopic parameters of aminoacetonitrile have never been compared to computed data. Currently, rotational, centrifugal distortion, and nuclear quadrupole coupling constants as well as electric dipole moment components can be evaluated with high precision and can provide a good reference for supporting the analysis of rotational spectra.[57,67] Therefore, the present investigation allows us to benchmark the accuracy obtainable by exploiting the strategy presented in Section 3. The comparison is reported in Table 2.

First of all, Table 2 shows that the computed rotational constants agree remarkably well with the experimental ones: the mean absolute percentage error (MAPE) is around 0.1%, in line with benchmark results available in the literature for molecules of similar size.[49,57,58,68,69] This is a further confirmation that our best-estimated CBS+CV equilibrium structure is very close to the actual equilibrium geometry of aminoacetonitrile. Moving to the centrifugal distortion constants, a similar agreement is observed for both the quartic and sextic terms, the MAPE being 2.1% and 2.5%, respectively. The error obtained

Table 2 Comparison of experimental and computed spectroscopic parameters for the main isotopologue of aminoacetonitrile in its vibrational ground state

| Constant | Unit | Experiment[a] | Best estimates[b] |
|---|---|---|---|
| $A$ | MHz | 30246.4909(9) | 30331.332 |
| $B$ | MHz | 4761.0626(1) | 4757.100 |
| $C$ | MHz | 4310.7486(1) | 4309.318 |
| $D_J$ | kHz | 3.0669(1) | 3.0576 |
| $D_{JK}$ | kHz | −55.295(1) | −55.809 |
| $D_K$ | kHz | 714.092(7) | 704.828 |
| $d_1$ | kHz | −0.67355(4) | −0.66398 |
| $d_2$ | kHz | −0.02993(1) | −0.02793 |
| $H_J$ | mHz | 9.56(3) | 9.894 |
| $H_{JK}$ | Hz | −0.1249(4) | −0.1261 |
| $H_{KJ}$ | Hz | −2.714(4) | −2.728 |
| $H_K$ | Hz | 53.27(2) | 51.17 |
| $h_1$ | mHz | 3.88(1) | 3.923 |
| $h_2$ | mHz | 0.476(6) | 0.4578 |
| $h_3$ | mHz | 0.0503(8) | 0.0523 |
| $\chi_{aa}$ ($NH_2$) | MHz | −2.77(4) | −3.088 |
| $\chi_{bb}$ ($NH_2$) | MHz | 1.20(9) | 1.158 |
| $\chi_{aa}$ (CN) | MHz | −3.48(3) | −3.552 |
| $\chi_{bb}$ (CN) | MHz | 1.50(6) | 1.472 |
| $\mu_a$ | D | 2.577(7) | 2.590 |
| $\mu_b$ | D | 0.575(1) | 0.567 |

Numbers in parentheses are standard errors and apply to the last significant digits. [a] Obtained from the analysis of all literature data. Dipole moments are taken from ref. 36. [b] Obtained as explained in Section 3.

for the quartic terms is in line with the expected uncertainty range of about 2–3%,[57,70] while the MAPE achieved on the sextic constants is well below the typical uncertainty of 5–7%.[57,70,71] Such small errors seem to indicate that aminoacetonitrile is rather rigid, but also that the centrifugal distortion analysis performed in ref. 33 is robust, as demonstrated by the large number of distortion terms determined.

Finally, there are two first-order properties that can be compared to experimental data, namely the nuclear quadrupole coupling constants of the nitrogen nuclei and the electric dipole moment components. The former have been determined during the analysis of the hyperfine structure performed by Brown *et al.*,[37] while the latter have been determined using Stark effect measurements.[36] For these quantities, the MAPE is found to be 4.7% on the quadrupole coupling constants and 0.9% for the dipole moments. The overall good agreement points out the quality of our *ab initio* calculations as well as the reliability of the rotational studies available in the literature.

### 4.3 Infrared spectrum

Aminoacetonitrile possesses 18 vibrational modes that can be classified – according to the irreducible representations of the $C_s$ point group – into 11 normal modes of $A'$ symmetry and 7 of $A''$ symmetry. At present, the knowledge of the mid-infrared spectrum of aminoacetonitrile relies on the works by Bak *et al.*[38] and Bernstein *et al.*[39] The former provided the first tentative assignment of each normal mode from the analysis of a gas-phase spectrum recorded at low resolution with an accuracy of *ca.* 1 $cm^{-1}$, while the latter reported the infrared spectrum obtained in a low-temperature matrix isolation experiment. Both studies were guided by low-level harmonic force-field calculations.

In this work, we have computed the position of each fundamental band by correcting the CBS+CV harmonic frequencies with the anharmonic contributions evaluated at the ae-MP2/cc-pCVTZ level, thus leading to a hybrid approach denoted as CBS + CV/MP2. Similar approaches have been used successfully in the past[49,50,72–74] and provided good results for species similar in size. Based on dedicated benchmark studies, we

Table 3 Harmonic frequencies computed at different levels of theory, anharmonic corrections, and anharmonic vibrational fundamentals (Hybrid) in comparison with experiments

| | CCSD(T) | | | | | | Anharm. corr. | | Experimental | |
|---|---|---|---|---|---|---|---|---|---|---|
| Mode | fc-pVTZ | fc-pVQZ | fc-CVTZ | ae-CVTZ | CBS | CBS+CV | MP2/ae-CVTZ | Hybrid | Low res.[a] | High res.[b] |
| $\nu_1$ | 3505 | 3514 | 3504 | 3511 | 3523 | 3530 | −152 | 3378 | 3367(1) | — |
| $\nu_2$ | 3078 | 3079 | 3078 | 3083 | 3082 | 3087 | −135 | 2952 | 2950(1) | — |
| $\nu_3$ | 2275 | 2283 | 2277 | 2285 | 2288 | 2296 | −42 | 2254 | 2236(1) | — |
| $\nu_4$ | 1674 | 1674 | 1674 | 1676 | 1675 | 1677 | −60 | 1617 | 1642(1) | — |
| $\nu_5$ | 1482 | 1482 | 1483 | 1484 | 1483 | 1485 | −39 | 1446 | 1444(1) | — |
| $\nu_6$ | 1369 | 1370 | 1370 | 1373 | 1371 | 1374 | −36 | 1338 | 1348(1) | — |
| $\nu_7$ | 1123 | 1123 | 1123 | 1122 | 1122 | 1124 | −38 | 1086 | 1077(1) | — |
| $\nu_8$ | 949 | 943 | 949 | 950 | 937 | 937 | −39 | 898 | 901(1) | 901.4(1) |
| $\nu_9$ | 849 | 845 | 849 | 851 | 842 | 843 | −32 | 811 | 790(1) | 790.95908(7) |
| $\nu_{10}$ | 560 | 562 | 561 | 563 | 563 | 565 | −6 | 559 | 558(1) | 556.56467(2) |
| $\nu_{11}$ | 211 | 211 | 211 | 212 | 211 | 212 | −1 | 211 | 216(1) | 210.575842(5) |
| $\nu_{12}$ | 3587 | 3597 | 3584 | 3592 | 3608 | 3616 | −168 | 3448 | 3431(1) | — |
| $\nu_{13}$ | 3122 | 3125 | 3123 | 3128 | 3129 | 3134 | −143 | 2991 | 2975(1) | — |
| $\nu_{14}$ | 1398 | 1396 | 1398 | 1400 | 1395 | 1397 | −37 | 1360 | 1331(1) | — |
| $\nu_{15}$ | 1203 | 1201 | 1204 | 1206 | 1200 | 1203 | −30 | 1173 | 1297(1) | 1160.(1) |
| $\nu_{16}$ | 895 | 894 | 896 | 897 | 893 | 895 | −11 | 884 | — | — |
| $\nu_{17}$ | 381 | 379 | 382 | 383 | 377 | 379 | −9 | 370 | 370(1) | 368.104657(3) |
| $\nu_{18}$ | 266 | 261 | 266 | 267 | 255 | 256 | −8 | 248 | 247(1) | 244.891525(3) |

Vibrational frequencies are expressed in $cm^{-1}$. Values in parentheses represent standard errors in unit of the last quoted digits. [a] Low resolution data from Bak *et al.*[38] [b] High resolution data from Melosso *et al.*[20] (below 500 $cm^{-1}$) or from this work (above 500 $cm^{-1}$).

 

expect that this hybrid approach is able to provide a solid base for reviewing the vibrational analysis, with a relative mean error better than 1% and maximum errors not exceeding 3%.[75–78]

Our best-estimated CBS+CV/MP2 predictions for the band centers of the 18 fundamental bands of aminoacetonitrile are provided in the third last column of Table 3 (denoted as Hybrid). By comparing these values with those reported by Bak *et al.*[38] and Melosso *et al.*,[20] an overall good agreement is noted, with only one exception. In fact, the feature lying at 1297(1) $cm^{-1}$ was assigned to the $\nu_{15}$ band in ref. 38, which is instead predicted to lie at 1173 $cm^{-1}$ by our calculations. This would result in a deviation of 124 $cm^{-1}$ and relative percentage error of about 10%, which is much larger than the average percentage error of the remaining fundamentals, which is around 1%. This discrepancy casts some doubt on the correct assignment of the $\nu_{15}$ vibrational mode by Bak *et al.*[38] The hypothesis of a wrong assignment is further supported by the detection of a weak feature around 1160 $cm^{-1}$ in the vibrational spectra recorded in this work. Therefore, we propose a new assignment for the $\nu_{15}$ band.

Concerning the $\nu_{16}$ band – not identified by Bak *et al.*[38] – our calculations predict an anharmonic intensity smaller than 0.001 km $mol^{-1}$, which makes this band impossible to be observed using the present experimental setup. Hence, our computed frequency should be used as best estimate for such fundamental band.

Table 3 also reports the harmonic frequencies at different levels of theory. It is noted that the CV contribution is small (on average 0.2%) and that the fc-CCSD(T)/cc-pVQZ level of theory provides results nearly converged to the CBS limit.

### 4.4 Ro-vibrational analysis of the $\nu_8$, $\nu_9$, and $\nu_{10}$ bands

In our previous work, we have recorded at high-resolution and analyzed the three strongest fundamentals that dominate the frequency region below 500 $cm^{-1}$, namely the $\nu_{11}$, $\nu_{17}$, and $\nu_{18}$ bands[20] (see Table 3 for the experimental band centers). Here, we investigate the region between 500 and 1000 $cm^{-1}$, where the three strongest features are the $\nu_8$, $\nu_9$, and $\nu_{10}$ bands. However, due to the greater congestion of the spectra and to the higher number of resonances that occur moving at higher energies, the present study is limited in terms of both assigned transitions and spectral analysis with respect to that of ref. 20. Yet, our ro-vibrational analysis is able to provide accurate band centers and a solid base for a more detailed study of these bands in the future.

All these three fundamentals show the typical structure of an *a*-type band, *i.e.* strong P and R branches with a less pronounced Q branch. To guide the analysis of the rotational structure of each band, spectral simulations have been obtained by combining the ground state spectroscopic constants from ref. 20 and a set of vibrational excited state parameters obtained from our computed band centers and vibration–rotation interaction constants. The spectral simulation has been performed with the PGOPHER package,[79] while the assignment procedure has been carried out using the graphical tools offered by the Loomis-Wood for Windows program.[80] Moreover, the correctness of the assigned transitions has been checked using the ground-state combination differences method and the MARVEL (Measured Active Rotational-Vibrational Energy Levels) software.[81] At the end of the assignment procedure, the spectral analysis has been performed using the SPFIT subroutine of the CALPGM suite of program[82] and employing a *S*-reduced Watson-type Hamiltonian for a semi-rigid nearly-prolate rotor.[83]

For the $\nu_{10}$ band – observed in the 534–577 $cm^{-1}$ range – we were able to assign and successfully analyze 1180 distinct transitions, which involve energy levels with $J$ and $K_a$ values up to 75 and 10, respectively. A sub-set of 147 transitions having high values for both quantum numbers (including all the $K_a$ = 11 transitions identified) have been discarded from the

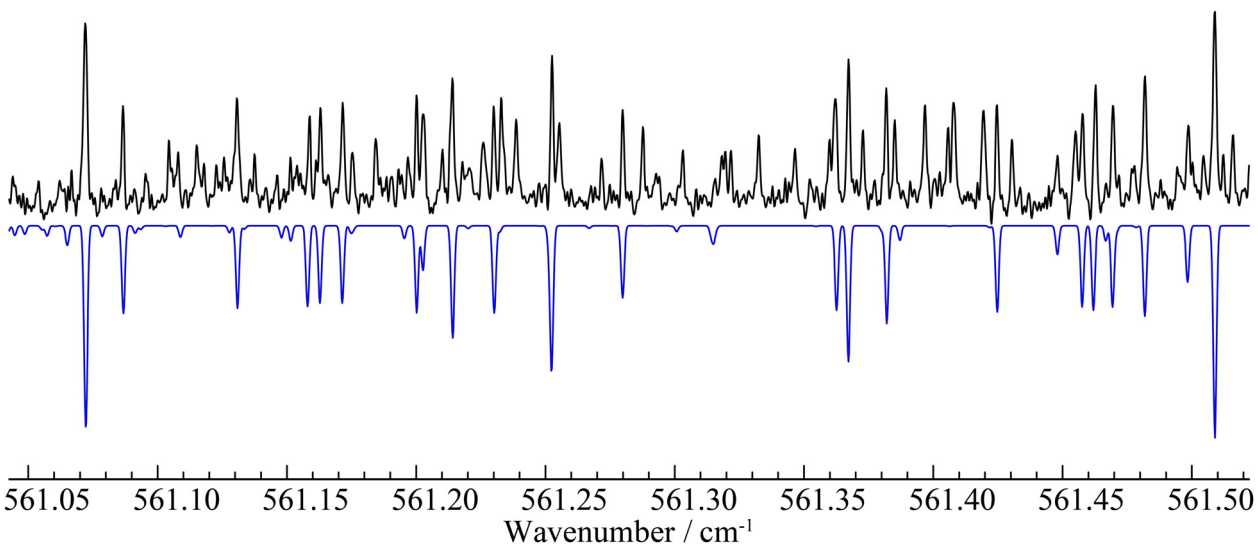


Fig. 2 Portion of the R branch of the $\nu_{10}$ band around 561 $cm^{-1}$. The experimental spectrum is shown in black, while a simulation based on our final spectroscopic constants is shown in blue. Unassigned features likely belong to hot-bands originating from the lowest-lying vibrational states.

analysis because they show deviations at least five times larger than the assumed experimental uncertainty of $2 \times 10^{-4}$ cm$^{-1}$. The root-mean-square (rms) error of the final fit is $2.6 \times 10^{-4}$ cm$^{-1}$, which is in line with the expected frequency accuracy. The experimental rotational constants of the $v_{10} = 1$ state have been obtained with good precision and the corresponding vibration–rotation interaction constants $\alpha_{10}^{A}$ = 382 MHz, $\alpha_{10}^{B} = -8.6$ MHz, and $\alpha_{10}^{C} = -7.9$ MHz agree very well with both the computed values ($\alpha_{10}^{A}$ = 386 MHz, $\alpha_{10}^{B} = -8.0$ MHz, and $\alpha_{10}^{C} = -7.5$ MHz) and those determined in a millimeter-wave study ($\alpha_{10}^{A}$ = 384 MHz, $\alpha_{10}^{B} = -8.6$ MHz, and $\alpha_{10}^{C} = -7.9$ MHz).[34] Moreover, the centrifugal distortion constants of the vibrational excited state are very similar to those of the ground state, which seems to indicate that the $v_{10}$ = 1 state is not strongly perturbed by another vibrational state. The band center, predicted at 560 cm$^{-1}$, is found to be 556.56467(2) cm$^{-1}$. Finally, we estimate that the *b*-type component of this band is at least 10 times weaker than the *a*-type component. Therefore, the unassigned features in this portion of the spectrum (see Fig. 2) belong mainly to hot-bands arising from low-lying energy states, *e.g.* $v_{11} = 1$, $v_{17} = 1$, $v_{18} = 1$.

The analysis of the $\nu_9$ band was slightly more problematic. In this case, we were able to assign a smaller number of transitions (707 lines in the 775–804 cm$^{-1}$ range, 623 of which were included in the analysis and 84 were discarded) whose maxima values of $J$ and $K_a$ are 47 and 7, respectively. A root-mean-square error of $7.1 \times 10^{-4}$ cm$^{-1}$ together with anomalous values obtained for $D_K$ and $d_2$ point out the existence of a moderate perturbation for the $v_9$ = 1 state. This is also supported by the large difference found between the theoretical $\alpha_9^A$ of 60 MHz and its experimental value of 204 MHz. The interaction occurs most likely with the $v_8 = 1$ and $v_{16} = 1$ states, but many other overtone and combination states can produce accidental degeneracy and thus perturb the $v_9 = 1$ energy levels. Given the difficulty in obtaining a thorough knowledge of the complete manifold of the vibrational excited states of aminoacetonitrile, we limit the present investigation to an effective and partial analysis. Still, the origin of this band has been determined at 790.95908(7) cm$^{-1}$ with good accuracy and compare well with our predicted value of 812 cm$^{-1}$. A good agreement is also obtained between our experimental $\alpha$ values for $B$ and $C$ ($\alpha_9^B = -22.0$ MHz and $\alpha_9^C = -11.8$ MHz) and those computed at the MP2 level ($\alpha_9^B = -22.5$ MHz and $\alpha_9^C = -15.9$ MHz). As last remark, we note that the tentative assignment made for this state by Kolesnikova *et al.*[34] in their pure rotational study is correct, as demonstrated by the similar vibration–rotation interactions constants derived ($\alpha_9^A$ = 194 MHz, $\alpha_9^B = -19.9$ MHz, and $\alpha_9^C = -12.2$ MHz).

The $\nu_8$ band was even more difficult to analyze. For this band, only 82 distinct lines corresponding to 168 transitions with $J \leq 21$ and $K_a$ values between 5 and 8 could be assigned safely. Attempts to derive a consistent set of spectroscopic constants and to search for further transitions – especially those with lower $K_a$ values – were unsuccessful. Presumably,

Table 4 Spectroscopic constants of the $\nu_{10}$ and $\nu_9$ bands

| Constant | Unit | $v_{10} = 1$ | $v_9 = 1$ |
|---|---|---|---|
| $E_{vib}$ | cm$^{-1}$ | 556.56467(2) | 790.95908(7) |
| $A$ | MHz | 30628.15(4) | 30450.1(2) |
| $B$ | MHz | 4752.461(2) | 4739.10(5) |
| $C$ | MHz | 4302.8854(8) | 4298.94(5) |
| $D_J$ | kHz | 3.0541(3) | 2.517(10) |
| $D_{JK}$ | kHz | −55.89(2) | −54.4(3) |
| $D_K$ | kHz | 748.3(4) | 512.(5) |
| $d_1$ | kHz | −0.6712(2) | −0.72(4) |
| $d_2$ | kHz | −0.02976(6) | −0.09(3) |
| No. of lines | | 1180 | 623 |
| $J$, $K_a$ max | | 75, 10 | 47, 7 |
| rms × 10$^3$ | cm$^{-1}$ | 0.26 | 0.71 |

Numbers in parentheses are standard errors and apply to the last significant digits.

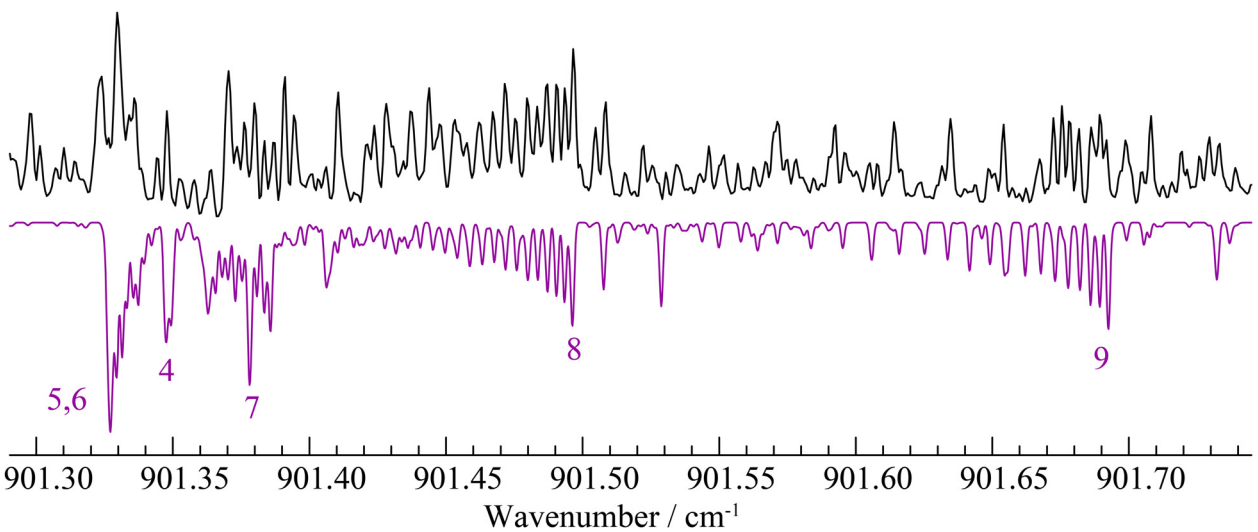


Fig. 3 Portion of the infrared spectrum around the band center of the $\nu_8$ band. The experimental spectrum (in black) is compared to a simulation of the Q branches (in violet). The numbers shown below each sub-branch correspond to the $K_a$ value involved in the transition.

 

the resonances affecting the $\nu_8 = 1$ state are much more pronounced due to its proximity to the $\nu_{16} = 1$ state, whose energy levels are unknown at present. In this case, we could only estimate the band center to be 901.4(1) $cm^{-1}$, a value that reproduces roughly the shape of the Q branches (see Fig. 3) and is in excellent agreement with our computed value of 898 $cm^{-1}$.

The spectroscopic constants determined from the analysis of the $\nu_{10}$ and $\nu_9$ bands are listed in Table 4, while the list of all the assigned transitions is provided in the ESI.†

## 5 Conclusions

The importance of aminoacetonitrile in astrochemistry demands for a deep knowledge of its spectroscopic properties. In this work, we presented the first thorough computational characterization of the structure and rotational/ro-vibrational spectra of aminoacetonitrile carried out by employing accurate quantum-chemical methods. This was accompanied by the determination of a semi-experimental equilibrium structure and the partial analysis of the three strongest vibrational bands observed between 500 and 1000 $cm^{-1}$.

As far as the molecular structure is concerned, the derived semi-experimental equilibrium geometry agrees very well with our best-estimated computational counterpart obtained by exploiting the CBS+CV composite scheme, thus confirming the accuracy of both approaches. Because of the close relationship between structure and physico-chemical properties, we recommend to use our newly determined geometry as reference for future spectroscopic studies. Focusing on the infrared spectrum, the CBS+CV harmonic frequencies combined with an accurate treatment of anharmonicity allowed us to predict very accurate positions for all fundamental bands, in good agreement with previous vibrational analyses.[38,39] Moreover, the anomalous large discrepancy between the computed position of the $\nu_{15}$ band and the experimental frequency attributed by Bak *et al.*[38] gave us the opportunity to point out the wrong experimental assignment and to re-assign this band to a feature observed at 1160 $cm^{-1}$ in our infrared spectra.

In addition to the theoretical characterization, we have recorded and analyzed three ro-vibrational bands observed in the 500–1000 $cm^{-1}$ range, namely the $\nu_8$, $\nu_9$, and $\nu_{10}$ bands. While the spectral analysis of the $\nu_{10}$ band was satisfactory and the determined spectroscopic constants are in line with those computed here and previous rotational studies,[34] the analysis of the $\nu_8$ and $\nu_9$ bands revealed the presence of strong perturbations. Still, the correct assignment of more than 2000 ro-vibrational transitions has been validated using the MARVEL algorithm and should provide a solid base for future investigations.

In general, the experimental/theoretical characterization of the molecular structure and spectroscopic properties of aminoacetonitrile provided in this work can be used to assist both astronomical observations and laboratory experiments concerning the important role played by this species in interstellar environments.

## Conflicts of interest

There are no conflicts to declare.

## Acknowledgements

This work has been supported by MIUR (PRIN Grant Number 202082CE3T) and by the University of Bologna (RFO funds). N. J. thanks the China Scholarships Council (CSC) for financial support. We would like to thank the AILES beamline staff for their assistance in data acquisition.

## Notes and references

1 K. Kvenvolden, J. Lawless, K. Pering, E. Peterson, J. Flores, C. Ponnamperuma, I. R. Kaplan and C. Moore, *Nature*, 1970, **228**, 923–926.
2 J. G. Lawless, K. A. Kvenvolden, E. Peterson, C. Ponnamperuma and C. Moore, *Science*, 1971, **173**, 626–627.
3 D. P. Glavin, J. L. Bada, K. L. Brinton and G. D. McDonald, *Proc. Natl. Acad. Sci. U. S. A.*, 1999, **96**, 8835–8838.
4 D. P. Glavin, A. D. Aubrey, M. P. Callahan, J. P. Dworkin, J. E. Elsila, E. T. Parker, J. L. Bada, P. Jenniskens and M. H. Shaddad, *Meteorit. Planet. Sci.*, 2010, **45**, 1695–1709.
5 D. P. Glavin, J. E. Elsila, A. S. Burton, M. P. Callahan, J. P. Dworkin, R. W. Hilts and C. D. Herd, *Meteorit. Planet. Sci.*, 2012, **47**, 1347–1364.
6 E. Nakamura, K. Kobayashi, R. Tanaka, T. Kunihiro, H. Kitagawa and C. Potiszil, *et al.*, *Proc. Jpn. Acad., Ser. B*, 2022, **98**, 227–282.
7 J. E. Elsila, D. P. Glavin and J. P. Dworkin, *Meteorit. Planet. Sci.*, 2009, **44**, 1323–1330.
8 K. Altwegg, H. Balsiger, A. Bar-Nun, J.-J. Berthelier, A. Bieler, P. Bochsler, C. Briois, U. Calmonte, M. R. Combi and H. Cottin, *et al.*, *Sci. Adv.*, 2016, **2**, e1600285.
9 J. M. Hollis, J. Pedelty, L. E. Snyder, P. R. Jewell, F. J. Lovas, P. Palmer and S.-Y. Liu, *Astrophys. J.*, 2003, **588**, 353.
10 L. E. Snyder, F. J. Lovas, J. Hollis, D. N. Friedel, P. Jewell, A. Remijan, V. V. Ilyushin, E. Alekseev and S. Dyubko, *Astrophys. J.*, 2005, **619**, 914.
11 A. Belloche, K. Menten, C. Comito, H. Müller, P. Schilke, J. Ott, S. Thorwirth and C. Hieret, *Astron. Astrophys.*, 2008, **482**, 179–196.
12 J. M. Hollis, F. J. Lovas and P. R. Jewell, *Astrophys. J.*, 2000, **540**, L107.
13 V. M. Rivilla, L. Colzi, I. Jiménez-Serra, J. Martn-Pintado, A. Megías, M. Melosso, L. Bizzocchi, A. López-Gallifa, A. Martínez-Henares and S. Massalkhi, *et al.*, *Astrophys. J., Lett.*, 2022, **929**, L11.
14 V. M. Rivilla, I. Jiménez-Serra, J. Martn-Pintado, C. Briones, L. F. Rodrguez-Almeida, F. Rico-Villas, B. Tercero, S. Zeng, L. Colzi and P. de Vicente, *et al.*, *Proc. Natl. Acad. Sci. U. S. A.*, 2021, **118**, e2101314118.
15 V. M. Rivilla, J. Martn-Pintado, I. Jiménez-Serra, S. Martn, L. F. Rodrguez-Almeida, M. A. Requena-Torres, F. Rico-Villas, S. Zeng and C. Briones, *Astrophys. J., Lett.*, 2020, **899**, L28.

16 A. Belloche, R. Garrod, H. Müller, K. Menten, I. Medvedev, J. Thomas and Z. Kisiel, *Astron. Astrophys.*, 2019, **628**, A10.
17 I. Jiménez-Serra, J. Martn-Pintado, V. M. Rivilla, L. Rodrguez-Almeida, E. R. Alonso Alonso, S. Zeng, E. J. Cocinero, S. Martn, M. Requena-Torres and R. Martn-Domenech, *et al.*, *Astrobiology*, 2020, **20**, 1048–1066.
18 R. Rubin, G. Swenson Jr, R. Benson, H. Tigelaar and W. Flygare, *Astrophys. J.*, 1971, **169**, L39.
19 C. Richard, A. Belloche, L. Margulès, R. Motiyenko, K. Menten, R. Garrod and H. Müller, *J. Mol. Spectrosc.*, 2018, **345**, 51–59.
20 M. Melosso, A. Belloche, M.-A. Martin-Drumel, O. Pirali, F. Tamassia and L. Bizzocchi, *et al.*, *Astron. Astrophys.*, 2020, **641**, A160.
21 A. Strecker, *Justus Liebigs Ann. Chem.*, 1850, **75**, 27–45.
22 G. Danger, F. Borget, M. Chomat, F. Duvernay, P. Theulé, J.-C. Guillemin, L. L. S. dHendecourt and T. Chiavassa, *Astron. Astrophys.*, 2011, **535**, A47.
23 F. Borget, G. Danger, F. Duvernay, M. Chomat, V. Vinogradoff, P. Theulé and T. Chiavassa, *Astron. Astrophys.*, 2012, **541**, A114.
24 A. Rimola, M. Sodupe and P. Ugliengo, *Phys. Chem. Chem. Phys.*, 2010, **12**, 5285–5294.
25 C. Chyba and C. Sagan, *Nature*, 1992, **355**, 125–132.
26 G. Danger, J.-B. Bossa, P. De Marcellus, F. Borget, F. Duvernay, P. Theulé, T. Chiavassa and L. dHendecourt, *Astron. Astrophys.*, 2011, **525**, A30.
27 G. A. Carvalho and S. Pilling, *Spectrochim. Acta A*, 2022, **267**, 120495.
28 R. T. Garrod, *Astrophys. J.*, 2013, **765**, 60.
29 C. He and M. A. Smith, *Icarus*, 2014, **238**, 86–92.
30 B. A. McGuire, *Astrophys. J., Suppl. Ser.*, 2022, **259**, 30.
31 J. MacDonald and J. Tyler, *J. Chem. Soc., Chem. Comm.*, 1972, **17**, 995.
32 M. Bogey, H. Dubus and J. Guillemin, *J. Mol. Spectrosc.*, 1990, **143**, 180–182.
33 Y. Motoki, Y. Tsunoda, H. Ozeki and K. Kobayashi, *Astrophys. J., Suppl. Ser.*, 2013, **209**, 23.
34 L. Kolesniková, E. Alonso, S. Mata and J. Alonso, *Astrophys. J., Suppl. Ser.*, 2017, **229**, 26.
35 C. Degli Esposti, L. Dore, M. Melosso, K. Kobayashi, C. Fujita and H. Ozeki, *Astrophys. J., Suppl. Ser.*, 2017, **230**, 26.
36 H. M. Pickett, *J. Mol. Spectrosc.*, 1973, **46**, 335–340.
37 R. Brown, P. Godfrey, A. Ottrey and J. Storey, *J. Mol. Spectrosc.*, 1977, **68**, 359–366.
38 B. Bak, E. Hansen, F. Nicolaisen and O. Nielsen, *Can. J. Phys.*, 1975, **53**, 2183–2188.
39 M. P. Bernstein, C. W. Bauschlicher Jr and S. A. Sandford, *Adv. Sp. Res.*, 2004, **33**, 40–43.
40 G. M. Chaban, *J. Phys. Chem. A*, 2004, **108**, 4551–4556.
41 M. Naganathappa and A. Chaudhari, *Int. J. Quant. Chem.*, 2011, **111**, 2064–2071.
42 J.-B. Brubach, L. Manceron, M. Rouzières, O. Pirali, D. Balcon, F. Kwabia-Tchana, V. Boudon, M. Tudorie, T. Huet, A. Cuisset and P. Roy, *WIRMS 2009*, 2010, pp. 81–84.
43 O. Pirali, V. Boudon, J. Oomens and M. Vervloet, *J. Chem. Phys.*, 2012, **136**, 024310.
44 O. Pirali, M. Goubet, T. R. Huet, R. Georges, P. Soulard, P. Asselin, J. Courbe, P. Roy and M. Vervloet, *Phys. Chem. Chem. Phys.*, 2013, **15**, 10141–10150.
45 M. Faye, M. Bordessoule, B. Kanouté, J.-B. Brubach, P. Roy and L. Manceron, *Rev. Sci. Instrum.*, 2016, **87**, 063119.
46 I. E. Gordon, L. S. Rothman, R. J. Hargreaves, R. Hashemi and E. V. Karlovets, *et al.*, *J. Quant. Spectrosc. Radiat. Transfer*, 2021, 107949.
47 V. M. Horneman, R. Anttila, S. Alanko and J. Pietila, *J. Mol. Spectrosc.*, 2005, **234**, 238–254.
48 C. Puzzarini, *J. Phys. Chem. A*, 2009, **113**, 14530–14535.
49 V. Barone, M. Biczysko, J. Bloino and C. Puzzarini, *Phys. Chem. Chem. Phys.*, 2013, **15**, 10094–10111.
50 V. Barone, M. Biczysko, J. Bloino and C. Puzzarini, *J. Chem. Phys.*, 2014, **141**, 034107.
51 C. Puzzarini, *Int. J. Quant. Chem.*, 2016, **116**, 1513–1519.
52 K. Raghavachari, G. W. Trucks, J. A. Pople and M. Head-Gordon, *Chem. Phys. Lett.*, 1989, **157**, 479–483.
53 D. Feller, *J. Chem. Phys.*, 1993, **98**, 7059–7071.
54 T. Helgaker, W. Klopper, H. Koch and J. Noga, *J. Chem. Phys.*, 1997, **106**, 9639–9646.
55 T. H. Dunning Jr., *J. Chem. Phys.*, 1989, **90**, 1007–1023.
56 D. E. Woon and T. H. Dunning Jr., *J. Chem. Phys.*, 1995, **103**, 4572.
57 C. Puzzarini, J. F. Stanton and J. Gauss, *Int. Rev. Phys. Chem.*, 2010, **29**, 273–367.
58 C. Puzzarini, J. Heckert and J. Gauss, *J. Chem. Phys.*, 2008, **128**, 194108.
59 I. M. Mills, *Molecular Spectroscopy: Modern Research*, ed. K. N. Rao and C. W. Matthews, 1972.
60 C. Møller and M. S. Plesset, *Phys. Rev.*, 1934, **46**, 618–622.
61 M. Piccardo, J. Bloino and V. Barone, *Int. J. Quantum Chem.*, 2015, **115**, 948–982.
62 P. Pulay, W. Meyer and J. E. Boggs, *J. Chem. Phys.*, 1978, **68**, 5077–5085.
63 *Equilibrium Molecular Structures: From Spectroscopy to Quantum Chemistry*, ed. J. Demaison, J. E. Boggs and A. G. Császár, CRC Press, Taylor & Francis Group, Boca Raton, FL, US, 2011.
64 M. J. Frisch, G. W. Trucks, H. B. Schlegel, G. E. Scuseria, M. A. Robb, J. R. Cheeseman, G. Scalmani, V. Barone, G. A. Petersson, H. Nakatsuji, X. Li, M. Caricato, A. V. Marenich, J. Bloino, B. G. Janesko, R. Gomperts, B. Mennucci, H. P. Hratchian, J. V. Ortiz, A. F. Izmaylov, J. L. Sonnenberg, D. Williams-Young, F. Ding, F. Lipparini, F. Egidi, J. Goings, B. Peng, A. Petrone, T. Henderson, D. Ranasinghe, V. G. Zakrzewski, J. Gao, N. Rega, G. Zheng, W. Liang, M. Hada, M. Ehara, K. Toyota, R. Fukuda, J. Hasegawa, M. Ishida, T. Nakajima, Y. Honda, O. Kitao, H. Nakai, T. Vreven, K. Throssell, J. A. Montgomery, Jr., J. E. Peralta, F. Ogliaro, M. J. Bearpark, J. J. Heyd, E. N. Brothers, K. N. Kudin, V. N. Staroverov, T. A. Keith, R. Kobayashi, J. Normand, K. Raghavachari, A. P. Rendell, J. C. Burant, S. S. Iyengar, J. Tomasi, M. Cossi, J. M. Millam, M. Klene, C. Adamo, R. Cammi, J. W. Ochterski, R. L. Martin, K. Morokuma, O. Farkas, J. B. Foresman and D. J. Fox, *Gaussian 16 Revision B.01*, Gaussian Inc., Wallingford CT, 2016.
65 J. F. Stanton, J. Gauss, M. E. Harding and P. G. Szalay, A. A. Auer, R. J. Bartlett, U. Benedikt, C. Berger, D. E. Bernholdt, Y. J. Bomble, O. Christiansen, F. Engel, M. Heckert, O. Heun, C. Huber,

T.-C. Jagau, D. Jonsson, J. Jusélius, K. Klein, W. J. Lauderdale, F. Lipparini, D. Matthews, T. Metzroth, L. A. Mück, D. P. O'Neill, D. R. Price, E. Prochnow, C. Puzzarini, K. Ruud, F. Schiffmann, W. Schwalbach, S. Stopkowicz, A. Tajti, J. Vázquez, F. Wang, J. D. Watts, and the integral packages MOLECULE (J. Almlöf and P. R. Taylor), PROPS (P. R. Taylor), ABACUS (T. Helgaker, H. J. Aa. Jensen, P. Jø rgensen, and J. Olsen), and ECP routines by A. V. Mitin and C. van Wüllen, *CFOUR. A quantum chemical program package*, 2016. For the current version, see https://www.cfour.de.

66 D. A. Matthews, L. Cheng, M. E. Harding, F. Lipparini, S. Stopkowicz, T.-C. Jagau, P. G. Szalay, J. Gauss and J. F. Stanton, *J. Chem. Phys.*, 2020, **152**, 214108.

67 V. Barone, S. Alessandrini, M. Biczysko, J. R. Cheeseman, D. C. Clary, A. B. McCoy, R. J. DiRisio, F. Neese, M. Melosso and C. Puzzarini, *Nat. Rev. Methods Primers*, 2021, **1**, 1–27.

68 C. Puzzarini, *Phys. Chem. Chem. Phys.*, 2013, **15**, 6595–6607.

69 S. Alessandrini, J. Gauss and C. Puzzarini, *J. Chem. Theory Comput.*, 2018, **14**, 5360–5371.

70 C. Puzzarini, G. Cazzoli and J. Gauss, *Chem. Phys.*, 2012, **137**, 154311.

71 R. Boussessi, N. Tasinato, A. Pietropolli Charmet, P. Stoppa and V. Barone, *Mol. Phys.*, 2020, **118**, e1734678.

72 V. Barone, M. Biczysko, J. Bloino, P. Cimino, E. Penocchio and C. Puzzarini, *J. Chem. Theory Comput.*, 2015, **11**, 4342–4363.

73 C. Degli Esposti, L. Dore, C. Puzzarini, M. Biczysko, J. Bloino, L. Bizzocchi, V. Lattanzi and J.-U. Grabow, *Astron. Astrophys.*, 2018, **615**, A176.

74 C. Puzzarini, N. Tasinato, J. Bloino, L. Spada and V. Barone, *Phys. Chem. Chem. Phys.*, 2019, **21**, 3431–3439.

75 C. Puzzarini, M. Biczysko and V. Barone, *J. Chem. Theory Comput.*, 2010, **6**, 828–838.

76 J. Bloino, M. Biczysko and V. Barone, *J. Chem. Theory Comput.*, 2012, **8**, 1015–1036.

77 I. Carnimeo, C. Puzzarini, N. Tasinato, P. Stoppa, A. Pietropolli Charmet, M. Biczysko, C. Cappelli and V. Barone, *J. Chem. Phys.*, 2013, **139**, 074310.

78 C. Puzzarini, J. Bloino, N. Tasinato and V. Barone, *Chem. Rev.*, 2019, **119**, 8131–8191.

79 C. M. Western, *J. Quant. Spectrosc. Radiat. Transfer*, 2017, **186**, 221–242.

80 W. Lodyga, M. Krkeglewski, P. Pracna and V. Urban, *J. Mol. Spectrosc.*, 2007, **243**, 182–188.

81 T. Furtenbacher, A. G. Császár and J. Tennyson, *J. Mol. Spectrosc.*, 2007, **245**, 115–125.

82 H. M. Pickett, *J. Mol. Spectrosc.*, 1991, **148**, 371–377.

83 J. K. G. Watson, in *Vibrational Spectra and Structure*, ed. J. Durig, Elsevier, Amsterdam, 1977, vol. 6, pp. 1–89.